University of Baghdad
College of Engineering
JOURNAL OF ENGINEERING

Journal of Engineering

journal homepage: www.jcoeng.edu.iq
Number 9 Volume 24 September 2018

Chemical, Petroleum and Environmental Engineering

Zeta Potential, Effective Membrane Charge and Donnan Potential for TiO_2 NF Ceramic Membrane

Ahmed Faiq Hassan Al-Alawy*
Professor
College of Engineering-University of Baghdad
E-mail: ahmedalalawy@yahoo.com

Amer Naji Ahmed Al-Naemi
Ph.D, Senior Chief of Engineers
Ministry of Science and Technology
E-mail: amer.alnaemi@yahoo.com

Mudhaffar Yacoub Hussein
Instructor
College of Engineering-University of Misan
E-mail:mudhhussein@yahoo.com

ABSTRACT

Nanofiltration (NF) ceramic membrane have found increasing applications particularly in wastewater and water treatment. In order to estimate and optimize the performance of NF membranes, the membrane should be characterized correctly in terms of their basic parameters such as effective pore radius (r_p) and equivalent effective thickness as well as effective surface charge (σ^s), the effective charge density (X^m) and Donnan potential (ψ_D). The impact of electrokinetic (zeta) potential on the membrane surface charge density, effective membrane charge density and Donnan potential at two different concentrations of the reference solutions 0.001, 0.01 M sodium chloride at various pH values from 3 to 9, and effective pore radius (r_p) for nominal 0.9 nm ceramic TiO_2 NF membrane were evaluated. Experiments were conducted at cross flow (1.0 m/s) using Microelectrophoresis technique for measuring membrane zeta potential, effective pore radius, and Donnan steric pore model (DSPM). The TiO_2 membrane isoelectric point (net membrane charge equals zero) was found at pH of 3.7, 3.5 for 0.001 and 0.01 M NaCl respectively. The results showed that the NF membrane zeta potential changes its sign from positive to negative after the isoelectric point. The evaluated effective pore radius was found to be equal to 0.56 nm by using (DSPM) and the membrane equivalent effective thickness equals to (2×10^{-6} m).

Key words: Donnan potential, Nanofiltration, Filtration potential, zeta potential, surface charge density

جهد زيتا وشحنة الغشاء الفعالة وجهد دونان لغشاء الترشيح السيراميكي النانوي

احمد فائق حسن العلوي
استاذ
كلية الهندسة- جامعة بغداد

عامر ناجي احمد
دكتوراه- خبير- رئيس مهندسين
وزارة العلوم والتكنولوجيا

مظفر يعقوب حسين
مدرس
كلية الهندسة- جامعة ميسان

*Corresponding author
Peer review under the responsibility of University of Baghdad.
https://doi.org/10.31026/j.eng.2018.09.02

Article accepted: 4/12/2017

الخلاصة

تطبيقات اغشية الترشيح النانوية اخذت تزداد خصوصاً في مجال معالجة المياه ومخلفات المياه. لغرض تحديد الاداء الافضل للأغشية النانوية، تحتاج الاغشية الى التوصيف الدقيق بدلالة العوامل الداخلة في تركيب الاغشية مثل نصف القطر الفعال (r_p) والسمك المكافئ للغشاء للفعال ($\Delta x/A_K$) وكذلك كثافة شحنة سطح الغشاء (σ^s)، كثافة الشحنة الفعالة (X^m)، وجهد دونان (ψ_D). تم دراسة وتقييم تأثير الجهد الكهربائي الحركي (جهد زيتا) على كثافة شحنة السطح، كثافة شحنة الغشاء وجهد دونان في تركيزين مختلفين (0.001 مولارية و 0.01 مولارية) لمحلول ملح كلوريد الصوديوم كمحلول لملح قياسي (1:1) في قيم دالة حامضية مختلفة من pH (3) الى pH (9)، وكذلك تم تحديد نصف القطر الفعال (r_p) للغشاء السيراميكي ثاني اوكسيد التيتانيوم يمتلك قطر مسامي اولي (رمزي) 0.9 نانومتر. قياس جهد زيتا تم باستخدام تقنية الترحيل الكهربائي (microelectrophoresis potential) وهي احدى الطرق الاساسية لقياس جهد زيتا واستخدام موديل رياضي (DSPM : موديل دونان للفراغ المسامي). تم اجراء التجارب بسرعة جريان 1 m/s (cross flow).

وضحت نتائج الدراسة بأن جهد زيتا للغشاء النانوي تتغير اشارته من الموجب الى السالب مع زيادة الدالة الحامضية. نقطة التعادل الكهربائي (صافي شحنة الغشاء تساوي صفر) وجدت في دالة حامضية (pH) تساوي 3.7 و 3.5 على التوالي. تم تحديد القطر الفعال للغشاء والذي وجد يساوي 0.56 nm باستخدام موديل (DSPM) والسمك المكافئ للغشاء الفعال ($\Delta x/A_K$) يساوي (2×10^{-6} m).

الكلمات الرئيسية: جهد دونان، الترشيح النانوي، جهد الترشيح، جهد زيتا، كثافة شحنة السطح.

1. INTRODUCTION

Nanofiltration is a membrane separation process, whose performance is intermediate between that of ultrafiltration and reverse osmosis, with a pore size of one nanometer **Eriksson, 1988**. The major advantages of membrane separation compared with other unit operations are less energy consumption, no phase change, no additive requirements, easy scale-up, integration into other separation process, higher selectivity towards monovalent ions, ability to retain small organic molecules, in addition to higher fluxes compared to reverse osmosis (RO) membranes **Musbah, et al., 2013.** Nanofiltration membrane process has a large range of industrial application spaces like medical devices, chemical, paper, semiconductor, purifying water and wastewater **Musbah, et al., 2013** textile and food engineering **Andrade, et al., 2014** as well as biotechnology and pharmaceutical application. Despite these advancements, a decline in performance of membrane over time results from membrane fouling **Zhu, and Elimelech, 1995**. Since the interaction of inorganic and organic colloidal substances with membrane surface in aqueous solution is dependent on the surface charge of the membrane **Song, and Elimelech, 1995**, estimation of electrokinetic (zeta) potential of membrane surface is critical to membrane fouling research. This characteristic has usually been overlooked in attempts to choose optimum operating conditions for different membrane separation processes **Song, and Elimelech, 1995**. A ceramic (NF) membrane acquires a surface charge when brought into contact with an electrolyte solution. This charge affects the distribution of ions at the solution-membrane interface; counter ions are attracted to membrane surface while co-ions are repelled from it. Based on that, a so-called electrical double layer (EDL) creates at the surface of membrane. The distribution of ions in electrical double layer can be characterized by different models, **Elimelech, et al., 1995**. Essential to all models of (EDL) is the idea of a shear plane (clipping plane). The plane separates the mobile part of (EDL) from the fixed part. The electrical potential at the plane of shear is called the electrokinetic (zeta) potential. Zeta potential is of significant importance to surface and colloid science since the potential of surface itself cannot be estimated experimentally **Elimelech, et al., 1995**. Zeta potential can be estimated from one of the

following measurements of electrokinetic microelectrophoresis potential, streaming potential electro-osmosis potential and sedimentation potential **Elimelech, et al., 1995**. The first two of these are the main for the most common methods and the last is seldom used. Inspection of the electrophoretic particles mobility (microelectrophoresis method) in suspension characterizes the net charge of particle by determining their velocity in an applied external electrical field, driving force is electrical force that leads to a mechanical motion **Herbig, et al., 2003**.

The performance of nanofiltration ceramic membranes in desalination depends on the complexity and concentration of ions of the electrolyte solution to be filtered, but also on the kind of membrane material. Nanofiltration ceramic membrane used is mostly made of metal oxides, that have amphoteric behavior so that the electric charge of the surface depends on the pH of the feed electrolyte solution **Condom, et al., 2004**. In addition to the zeta potential (electrostatic) influence, the size of species to be filtered is also another parameter that should be considered, especially if the aqueous solution complexed cations with organic or mineral materials. Composite or asymmetric membranes is a significant and common kind of membrane that is made from several sublayers having various transport properties. Since this asymmetric membrane may be formed from the various material the overall performance may be correlated sharing each of various layers. As an example, if one sublayer offers high salt rejection (as generally occurs with effective layers of membranes like nanofiltration and reverse osmosis membranes), the permeate solution has concentration much lower than the feed solution. Usually, the lower or higher concentration of indirect impacts in the parameters measured for the asymmetric membrane is correlated to the various structures and transport properties of the sublayers formation the asymmetric membrane **Benavente, et al., 2000**. The membrane charge depends on isoelectric point (i.e.p) of the membrane and the solution pH. Many researchers have used zeta (electrokinetic) potential of the membrane as a key parameter to investigate the fouling characteristics of various membranes **Salgın, et al., 2006**. In most published investigations on the electrokinetic (zeta) potential of the membrane, the salt solution NaCl or KCl are used to simplify the analysis of data **Lanteria, et al., 2011**. In this study, the calculation of effective pore size was done, results will be shown using microelectrophoreses potential measurements to calculate the membrane surface charge density (mC/m^2), effective membrane charge (mol/m^3) and Donnan potential (mV) at different concentration of single salt (0.001 and 0.01 M NaCl) and different pH (3-9).

2. THEORY

According to **Al-Naemi, 2013 and Peeters, et al., 1999**, the correlation between the net surface charge density (σ^s) of the membrane and the zeta potential of the membrane for low potentials (generally below 50 mV) can be estimated by using the simplified Grahame equation:

$$\sigma^s = \frac{\varepsilon_r \varepsilon_o \zeta}{K^{-1}} \quad (1)$$

In **Eq. (1)**, σ^s is surface charge density, (C/m^2), ε_r is relative permittivity of water (78.5), ε_o is the permittivity of free space (8.854 X 10^{-12} C.V^{-1}.m^{-1}), ζ is the zeta potential (V) and K^{-1} is the Debye length (m), in which:

$$K^{-1} = \sqrt{\frac{\varepsilon_r \varepsilon_o K_B T}{2000 e^2 I N_A}} \quad (2)$$

In **Eq. (2),** N_A is the Avogadro's number (6.02×10^{23} mol^{-1}), K_B is the Boltzmann constant (1.38×10^{-23} J/K), T is the absolute temperature (K), I is the ionic strength and e is the magnitude of the electron charge (1.6022×10^{-19} C) where **Jawor, and Hoek, 2009**:

$$I = \frac{\Sigma z_i^2 c_i}{2} \quad (3)$$

In **Eq. (3)**, z_i is the ion valiancy and c_i is the ion concentration. For aqueous solution of NaCl, K^{-1}= 0.3 nm at 1.0 M and 30.4 nm at 10^{-4} M. The active membrane surface fixed charge density X^m shows the concentration of electrically charged groups on the surface of membrane. This parameter can be determined from converting the surface charge density $\sigma^s$of membrane to units of concentration by assuming that the surface charge of membrane is symmetrically spreaded in the void volume of pores; as represented in the following equation:

$$X^m = \frac{2\sigma^s}{r_p F} \quad (4)$$

Where: X^m is the electrical charged groups concentration on the surface of the membrane (mol/m^3), σ^s is the electrical charge on the surface of the membrane (C/m^2), r_p is effective membrane pore radius (m) and F is the Faraday constant (964867 C/mol).

The electrostatic repulsion and interaction between membrane surface charge and ions of the solute represent one of the mechanisms which could demonstrate the rejection behavior of ions in nanofiltration membrane. This mechanism can be demonstrated by the Donnan potential **Dukhin, et al., 2004**. Based on the **Schaep, and Vandecasteele, 2001**, there is a variation between the ionic concentrations in the membrane compared to these in the bulk solution. The same charge sign as the fixed charge of the membrane surface (co-ions) is lower in the membrane phase, while, the opposite charge sing to the fixed charge of the membrane (counter-ions) concentration is higher in the membrane phase than the bulk solution. Based on this difference, an electrical potential is built-up at the membrane interface transport of the counter ions to the solution phase and the counteract of the transport of co-ions to the membrane phase. This potential is well-known the Donnan potential when a pressure gradient across the membrane is applied, the impact of the Donnan potential is to repulse the same charge sign as a fixed charge of the membrane surface (co-ions) from passing through the membrane. In order to attain the electroneutrality requirement of the system, the ions of opposite charge sign to the fixed charge of the membrane are rejected also and salt retention happens. This behavior is called the Donnan equilibrium formalism.

Peeters, et al., 1999 demonstrated that the estimation of the Donnan potential depends basically on the effective fixed charge concentration in the membrane, concentration of solute and valence of both co-ion and counter-ions. The standard equation which describes the Donnan potential ($\Delta\psi_{Don}$) for the ideal solution is given by **Schäfer, et al., 2007** :

$$\Delta\psi_{Don} = \frac{R_g T}{z_i F} In\left(\frac{a_i}{a_i^m}\right) \quad (5)$$

Where, a_i and a_i^m represent the activity of ion i in the bulk solution and inside the membrane pores respectively. This equation is known as the Nernst equation. The ion i in Eq. (5) might indicates either the anion or the cation of the solute (such as Cl^- or Na^+ in case of using a sodium chloride (NaCl) as a background electrolyte). Literatures show that there are few approaches which can be used to estimate the value of the Donnan potential. However all these methods depend on estimation of the effective fixed charge density of the membrane surface. According to, Theorell, Meyer and Siever (TMS) model **Schaep, and Vandecasteele, 2001**; the Donnan potential for 1:1 electrolytes can be calculated as follows :

$$\Delta\psi_{Don} = \frac{R_g T}{F}\left(In\frac{c_2}{c_1} In\frac{\Phi X+\sqrt{4c_2^2+\Phi^2X^2}}{\Phi X+\sqrt{4c_1^2+\Phi^2X^2}}\right) \quad (6)$$

Here, $\Delta\psi_{Don}$ is Donnan potential (V), R_g is the universal gas constant (8.314 $J.mol^{-1}.K^{-1}$), c_1 is the concentration of ion at feed side (mol/m^3), c_2 is the concentration of ion at the permeate side (mol/m^3), X is the membrane effective charge density (mol/m^3) and Φ is a parameter indicating the characterstics of the electrolyte-membrane pair considered, and basically depends on the kind the electrolyte concentration and the electrolyte. Φ in the TMS model is always equal to 1 **Schaep, and Vandecasteele, 2001**. The Donnan equilibrium must be obtained in order to satisfy the electro-neutrality conditions of the system; this can be written as follows:

$$z_f c_f + \sum_{i=1}^{N} z_i c_i = 0 \quad (7)$$

where (f) indicates the strongly bound on the pore wall.

Based on the Boltzmann distribution, the ion concentration distribution c_i of valence Z_i can be written as **Davies, et al., 1961**:

$$c_i = C_{i,bulk}\, exp\left(-\frac{z_i F}{R_g T}\Delta\psi_{Don}\right) \quad (8)$$

By selecting the reference ion, the famous expression for the Donnan potential of the membrane surface (in volt) can be determined based on the bulk concentration C_i, the bulk of every ion and the effective membrane fixed charge concentration from substituting and solving of **Eq.(7)** and **Eq. (8)** as follows, **Al-Naemi, 2013 and Chein, et al., 2009**:

$$\Delta\psi_{Don} = \frac{R_g T}{F} sinh^{-1}\left(\frac{z_f X^m}{2C_{i,bulk}F}\right) \quad (9)$$

Eq. (9) is applied only for 1:1 electrolytes with bulk concentration of C_i, bulk (mol/1) and valance z_f **Chein, et al., 2009** whereas the effective charge density X^m (mol/m^3) can be determined from **Eq.(4)** according to the value of the membrane surface charge density σ^s (c/m^2).

The hindered nature of solute (glucose) transport in the extended Nernst-Planck (ENP) equation gives the ability of estimated (r_p) of the ceramic NF (TiO_2) membrane. Bowen et al. **Bowen, et al., 1998** confirmed that the rejection evaluations of an uncharged solute give the characterization of a membrane in terms of two factors: the effective ratio of membrane thickness to porosity ($\Delta x/A_k$) and the effective pore radius (r_p). The ENP : extended Nernst-Plank equation composes the main for desa cription of solute transport through nanofiltration

membrane **Bowen, et al., 1998**. It characterizes transport in terms of diffusion under the action of solute flow or pressure gradient, migration under the effect of an instantaneously rising electric field, and the action of the solute concentration. The extend Nernst-Plank equation has been modified by coethe fficient of hydrodynamics in order to take the impact of finite pore size on together convection and diffusion into account. The nanofiltration membrane is usually considered as a package of identical pores which diameter is much less than their length, so that both ions flux and volume flux can be considered as one dimensional **Garba, et al., 1999**. By using molar units for the electrochemical potential and base on the approximation of no direct coupling between ion fluxes, Bowen **Bowen, and Mohammad, 1998**, described the transport equation for ion fluxes through pores of nanthe ofilteration membrane as follows :

$$J_i = -D_{i,p}\frac{dc_i}{dx} - \frac{Z_i c_i D_{i,p}}{R_g T} F \frac{d\psi^m}{dx} + K_{i,c} c_i V \quad (10)$$

The first term on the right hand side of Eq. (10) represents transport due to diffusion, the second term represents the electric field, and the third term represents the convection respectively, where :

$J_i$is the flux of ion i (mol/m^2.s), $D_{i,p}$ is the concentration of ion i in membrthe ane (mol/m^3), x is the distance normal to membrthe ane (m), Z_i is the valance of ion i (dimensionless), F is the Faraday constant (C/mol), R_g is the real gas constant (J/mol.K), T is the absolute temperature (K), ψ^m is the electrical potential of the membrane (V), $K_{i,c}$ is the ionic hindrance coefficient for convection (dimensionless) and V is the solute velocity (m/s). The thickness divided by porosity and the pore size can be estimated by using the permeation test of the uncharged solute **Ahmad, and Ooi, 2006**. For neutral or uncharged solutes (such as glucose), there will be no term of electrostatic thus, only diffusion and convection flows influence the transport of solutes inside the membrane. So, the solute flux can be written as follows :

$$J_i = -D_{i,p}\frac{dc_i}{dx} + K_{i,c} c_i V \quad (11)$$

Rahi, et al., 2010 qualified glucose as the most considerable neutral sugar. While **Bowen, and Mohammad, 1998** showed that in such narrow pores as these in NF membrane, the glucose has an acceptable range of rejection. In order to get an expression for the rejection of solute, **Eq. (11)** is integrated across the membrane with solute concentration at (x = 0) that are on the bulk side of the membrane and ($\Delta x = x$) that is on the permeate side of the membrane.

Eq. (11) can be written in terms of rejection (R) as follows, **Al-Naemi, 2013** ;

$$R_i = 1 - \frac{C_i^{permeat}}{C_i^{feed}} = 1 - \frac{K_{i,c}\emptyset}{1-\exp(-pe*)[1-\emptyset K_{i,c}]} \quad (12)$$

Where :

pe* is the Peclet number, that can be described as follows :

$$pe^* = \frac{K_{i,c}}{K_{i,d}} \frac{J_v \Delta x}{D_{i,\infty} A_K} \quad (13)$$

Where :

$K_{i,d}$ is the hindered coefficient for diffusion (dimensionless), J_v is the permeate volume flux ($m^3/m^2.s$), $D_{i,\infty}$ is the molecular diffusion coefficient of ion i at infinite dilution (m^2/s) and A_K is the porosity of membrane (dimensionless). The hindered diffusivity of ion i ($D_{i,p}$) can be estimated as follows:

$$D_{i,p} = D_{i,\infty}.K_{i,d} \quad (14)$$

∅ is steric partitioning coefficient calculations for the sieve influence due to the intrinsic porosity of the NF membrane. The steric partitioning coefficient is restricted between 0 and 1. From the definition of the steric portioning coefficient for cylindrical pores, it can be written as follows **Bowen, et al., 2002** :

$$\emptyset_i = (1-\lambda_i)^2 \quad (15)$$

Here λ_i is the ratio of stocks radius of ion i (or solute) to the effective pore radius of the membrane. The hydrodynamic coefficients $K_{i,c}$ and $K_{i,d}$ depend on the solute to pore size ratio, λ_i in which **Ahmad, and Ooi, 2006**:

$$\lambda_i = \frac{r_i}{r_p} \quad (16)$$

r_i is the Stock radius of ion i (or solute) (m) and r_p is the membrane effective pore radius (m).
It should be noticed that $K_{i,c,}$ and $K_{i,d}$ are not dependent only on (ratio of solute to pore size) (λ_i), but also on the radial position within pothe re. However, the impact of the finite pore size on both convection and diffusion can be accurately evaluated using the values of ($K_{i,c}$ and $K_{i,d}$) at the pore center only, **Deen, 1987**.
Moving of solute in free solution encounters a drag force exerted by the solvent, so when solutes move in restricted spaces (pores of the membrane), the drag is modified and the transport may be considered to be hindered **Silva, et al., 2009**. Stokes radius of ion (r_i) can be determined from the well-known Stocks-Einstein equation as follows **Ahmad, and Ooi, 2006**.

$$r_i = \frac{K_B T}{6\pi\eta D_{i,\infty}} \quad (17)$$

Where, K_B is the Boltzmann constant (1.38×10^{-23} J/K), while T and η are the absolute temperature (K) and the dynamic viscosity of the solution (Pa.s) respectively. The diffusion coefficient of the molecular of the glucose solute at infinite diffusion equals to 0.69×10^{-9} (m^2/s). Thus by applying **Eq. (17)**, the stocks of glucose solute equal to 0.31×10^{-9}(m). The magnitude of the finite pore size acts on the convection and diffusion solute fluxes inside pores depend essentially on pore geometry. For a cylindrical geometry (supposing that they can be applied to charge species) the values of $K_{i,c,}$ and $K_{i,d}$ can be determined as a function of ionic radius/ pore radius ratio for ($0 < \lambda_i \leq 0.8$) as follows **Bowen, et al., 2002** :

$$K_{i,d} = 1.0 - 2.3\left(\frac{r_i}{r_p}\right) + 1.154\left(\frac{r_i}{r_p}\right)^2 + 0.224\left(\frac{r_i}{r_p}\right)^3 \quad (18)$$

$$K_{i,c} = (2 - \emptyset)(1.0 + 0.054\left(\frac{r_i}{r_p}\right) - 0.988\left(\frac{r_i}{r_p}\right)^2 + 0.441\left(\frac{r_i}{r_p}\right)^3 \quad (19)$$

The Hagen-Poiseuille equation provides the relationship between the applied pressure across the membrane and the pure water flux (J_w) as follows **Ahmad, and Ooi, 2006** :

$$J_w = VA_K = \frac{r_p^2 P}{8\mu(\frac{\Delta x}{A_K})} \quad (20)$$

P is the applied pressure (pa) and μ is the dynamic viscosity of the solution (pa.s).

3. EXPERIMENTAL WORK

3.1 Membranes

Tubular nanofiltration ceramic membrane (Inopor® single channel, produced by GmbH Veilsdrof – Germany) was used. This is structured so that the particles of inorganic oxide comprising the inner membrane surface layer of the circular ceramic tube determine the nominal pore size of the membrane surface. The surface layer of the membrane is supported by several porous ceramic tubes that can be manufactured from the alternative or same metal oxide. A membrane having 0.9 nm (0.9×10^{-9} m) nominal pore size was selected for the present research and this is classified as NF membrane. The effective inner surface of the membrane is formed of a layer of (TiO_2) that is deposited on a porous alumina support having a pore size of 0.05 µm. The dimensions of the membrane are: 7 mm i.d, 10 mm o.d and 190 mm in length and the area of permeate for circular membrane tube is about 4.176×10^{-3} m^2.

3.2 Filtration Experiments

A solution of sodium chloride (NaCl) was prepared by using a solid dried analytical NaCl (Aldrich U.K.) with very pure water (BOECO, Filter Cartridge BOE80910 type: 50136990, Thermo Fisher, Germany) with an organic contamination less than 0.03 (ppm) and a resistivity of approximately 18 MΩ cm^{-1}. A feed solution of NaCl was prepared with two different concentrations (10^{-3} and 10^{-2} M NaCl) that were run in the cross flow nanofiltration system schematically shown in **Fig. 1**. The basic components glass container (5 liters), a magnetic stirrer (Model No.HS-30, Human Lab Instrument Co. Korea), a centrifugal pump (BALDOR. RELIANCE, Super-E Motot. CAT.No.CEM 3354, SPEC 35AOIZPBOZGI U.S.A) flexible piping and different fittings, a cylindrical module, st:st valves. The flow rate of the permeate was determined by using a measuring cylinder put on the top of a balance with high accuracy and stopwatch. Different pieces of piping, a flow meter, valves and connectors complete the instruments. To estimate the pore size for the active surface of the membrane, experiments with uncharged solute (glucose) were carried out with transmembrane pressure (TMP) different from (1 to 15 bar). The concentration of the solute (glucose) in the permeate were monitored. The rejection was evaluated as a function of the flux. A solution of glucose was used with a concentration of 500 (ppm). In this study, every experiment of filtration was repeated at least twice to achieve excellent reproducibility. The filtration was worked at a cross flow velocity of (1.0 ms^{-1}).

3.3 Membrane Characterization

A sample of ceramic nanofiltration membrane was cut to a length of approximately 3 mm to allow investigation of the membrane surface by using an SEM: scanning electron microscope (FEI QUANTA 200, Prague, Czech Republic) worked at an accelerating voltage of (20-30) KV. Furthermore, an elemental analysis was taken by using an (EDXS: energy dispersive X-ray spectrometer).

3.4 Microelectrophoresis Potential Analyzer (Calculation of Zeta Potential)

The electrokinetic (zeta) potential of the membrane was measured by using microelectrophoresis method. The electrophoretic mobility of the flour particles was measured (Zeta plus, Zeta potential and particle size, Analyzer, 21521, Brookhaven Instruments, U.S.A.) at two various ionic strength of sodium chloride (10^{-3} and 10^{-2} M NaCl). The oxide suspension (ground particles) was adjusted in the range of (3-9) using 0.1 M NaOH or HCl where appropriate and the zeta potential of the particles was calculated using the Helmholtz-Smoluchowski equation **Narong, and James, 2006** :

$$\zeta = \frac{\mu U}{\varepsilon \varepsilon_o} \tag{21}$$

Here μ is the viscosity of the solution, U is the electrokinetic mobility of the particle ($\frac{u}{E}$) and u is the particle velocity in an electrical field of strength E. The microelectrophoresis measurements need particles of the membrane material that can often only be achieved by destroying and crushing the membrane. The effective diameter of the membrane powder used is approximately (500 nm) as shown in **Fig.2**. The effective diameter was measured using particle size measuring device and zeta potential (Zeta plus, Zeta potential and particle size, Analyzer, 21521, Brookhaven Instruments, U.S.A.).

4. RESULTS and DISCUSSION

4.1 SEM and EDXS of Ceramic NF Membrane

The (SEM) cross-section image of tubular (NF) ceramic membrane is shown in **Fig.3**. The ceramic membrane used in this work is an asymmetric (composite) thin layer of titanium dioxide and aluminum oxide which can be seen obviously. Three various membrane support layers the outer of that is formed of sintered aluminum oxide. **Fig.4** shows the specific spectrums of the effective surface of the NF ceramic membrane determined using (EDXS).

4.2 Determination of Pore Size

The pore size of the membrane is an important NF membrane characteristic to determine the effect of the solute size on its rejection. To calculate the membrane pore size, the Donnan steric pore partitioning model (DSPM) was used. Experiments of filtration were carried out with glucose. The solute radius was estimated from diffusion coefficients using stokes Einstein **Eq. (17)** to be 0.31 nm. **Wang, et al., 1995**. The rejection of solutes was determined as a function of the flux. For 0.9 nm NF ceramic membrane the results are shown in **Fig.5**.

The experiment of rejection for an uncharged solute (glucose) at a concentration of 500 (ppm) **Johan, et al., 1998** was conducted using the tubular ceramic titanium dioxide NF membrane at various applied pressure limited from 1.0 to 8 bars. The glucose rejection was determined based on its bulk permeate concentrations **Eq.(13)**. The concentration of glucose was analyzed using the glucose analyzer (Model: GL6 ANALYSER), the assay Kit being supplied by Analox Instruments Ltd, UK. **Fig.6** shows the flux of permeate (m/s) versus the applied pressure/ 8 μ (s^{-1}) for the ceramic NF titanium dioxide membrane. According to the Hagen-Poiseuli equation, the resulting slop ($r_p^2/\Delta x$) from **Fig.6** equals to 5.24×10^{-14}. Subsequently, the active membrane thickness (Δx) can be easily measured from the determined slope as functiona of the measured effective pore radius $\Delta x = (r_p^2 A_K/slope)$. **Fig.5** shows the glucose rejection of glucose with the permeate flux of glucose (m/s) for the ceramic NF titanium dioxide membrane. Data of the glucose rejection show, as predictable, that the retention increases with permeate flux increase. Using (Microsoft`s spreadsheet solver^{TM} add in, Microsoft Excel^{TM}) and substituting **Eq. (13), (15), (16), (17), (18)** and **(19)** into **Eq. (12)**, and solving to evaluate the effective membrane pore radius of the NF titanium dioxide membrane according to the resulting retention value of the glucose. The active layer thickness of the effective membrane surface can be substituted in terms of effective membrane surface pore radius that was also stated in the slope of **Fig.6**. The determined result of the effective pore radius for the existent tubular ceramic titanium dioxide membrane using the Donnan steric pore model showed that the effective pore radius of the present tubular NF ceramic titanium membrane was found equal to 0.56 nm. After knowing the value of effective pore radius, the active layer of the membrane can then be easily determined from the slope equation declared in **Fig.6**. The determined effective layer thickness (Δx) of the ceramic membrane titanium dioxide based on the Donnan steric pore model was equal to 0.8×10^{-6} (m) and the ratio of effective membrane length (thickness) to porosity ($\Delta x/A_k$) was approximately equal to 2×10^{-6} m. The effective estimated results of the effective ceramic (TiO_2) radius and active membrane thickness from applying this model are in agreement with the result stated by **Bowen, and Mukhtar, 1996**.

4.3 Influence of Electrolyte Concentration and pH on the Electrokinetic Potentials of Membrane

Microelectrophoresis potential measurements have been carried out to measure the zeta potential of the membrane in order to characterize the kind and value of the surface charge for circular tube ceramic titanium dioxide nanofiltration membrane. The zeta potential was measured from microelectrophoresis technique for a background electrolyte concentration of 10^{-3} and 10^{-2} M sodium chloride (NaCl) over an extent of pH magnitudes from 3 to 9.

Fig. 7 shows a sample of the zeta potentials estimated from microelectrophoresis method at pH magnitudes 3, 3.7, 4, 5, 6, 7, 8 and 9 respectively for a background electrolyte of sodium chloride 0.001 M (NaCl). **Fig. 8** shows a sample of the zeta potentials estimated from microelectrophoresis method at pH magnitudes 3, 3.5, 4, 5, 6, 7, 8 and 9 respectively for a background electrolyte of sodium chloride 0.01 M (NaCl). **Fig. 9** shows a plot of the evaluated zeta potential across a range of pH values from 3 to 9 using 0.001 and 0.01 M of sodium chloride as a background electrolyte. The influence of pH on the zeta (electrokinetic) potential as

a function of increasing electrolyte concentration and pH of NaCl is shown in **Fig.9** for two various concentrations (10^{-3} and 10^{-2} M sodium chloride).

The results show that the zeta (electrokinetic) potentials of the membrane particle used in this research are positive at pH (3) being found (8.52) and (3.79) mV for 10^{-3} and 10^{-2} M sodium chloride, respectively. The isoelectric point (i.e.p) was found between pH (3.7) and (3.5). Some researchers **Mullet, et al., 1997** have attributed changes in isoelectric point to the adsorption of cations and anions on the surface of the membrane. The estimated result of the zeta potential is in agreement with the result stated by **Al-Naemi, 2013** at pH 3.8 – 4 and concentration 0.01 M NaCl, that varies slightly between (3.5) and (3.8) due to changes in properties of the surface of the material caused by the technique of measuring (streaming potential). **Narong, and James, 2006** found that (i.e.p.) for UF ceramic membrane was at pH value of (3.3), for concentration 0.01M NaCl which corresponded the result obtained in this study. When pH is increased, the zeta potentials begin to be more negative, with the maximum values of the zeta potential being found at pH (9) that is equal to (-35) mV, (-32.5) mV at $10^{-3}$and 10^{-2} M sodium chloride respectively. It is seen from those results that at fixed NaCl concentration, the sign of the zeta potential can be significantly changed by varying (pH), whereas at fixed pH the changes in the concentration of salt do not have such a great impact. This investigation is in agreement with **Moritz, et al., 2001**.

4.4 Determination of Donnan Potential

This section consists of three main parts; the first one is related to the evaluation of charge density of the membrane particles surface whereas the second part and third part are related to the evaluation of the effective fixed charge density of membrane particles and the Donnan potential.

4.4.1 Determination of Membrane Particles Surface Charge Density

The net particle surface charge density or the electrokinetic particles surface charge density (σ^s) at the plane shear (clipping) can be determined from the electrokinetic (zeta) potential data depending on the Gouy-Chapmman theory. In the case of relatively low potential with less than 50 mV **Pessarakli, 1999**, and depending on the electrical double layer, the correlation between the zeta potential and the surface charge density at the hydrodynamic shear plane is given in **Eq. (1)**. The magnitude of the Debye length (K^{-1}) for (1:1) electrolytes (for example NaCl) can be estimated from **Eq. (1)**. The membrane particles surface charge density can be calculated from Graham equation by substituting the magnitudes of zeta potential which were previously evaluated for each (pH) value (**Fig. 10**) at 0.001 and 0.01 M NaCl. **Fig. 10** shows a plot of the estimated surface charge density (mC/m^2) across a range of pH magnitudes from (3 to 9) using 0.001 and 0.01 (NaCl) respectively, as a background electrolyte. **Fig. 11** shows a plot of the estimated membrane effective charge density (mol/m^3) across a range of pH magnitudes from (3 to 9) using 0.001 and 0.01 (NaCl) respectively, as a background electrolyte. **Fig. 12** shows a plot of the estimated Donnan potential (mV) across a range of pH magnitudes from (3 to 9) using 0.001 and 0.01 (NaCl) respectively, as a background electrolyte.

The membrane particles zeta potentials that can be evaluated from electrokinetic measurements give information concerning the net charge of the particle surface and thereby, membrane

particles charge density (σ^s) can be determined from data of zeta potential depending on the theory of Gouy-Chapman and Graham **Eq. (1)**. The results from **Fig. 10** show the as the pH magnitudes increase, the particles surface charge density begins to be more negative being found at pH (9) that is equal to (-2.26 mC/m^2), (-6.66 mC/m^2) at 0.001, 0.01 M NaCl respectively, while, at a pH of 3 the particles surface density becomes positive with a value of (0.55 mC/m^2), (0.78 mC/m^2) for 0.001 and 0.01 M respectively; that quite the same behavior of related zeta potential. The outcomes also show that the (pH) magnitudes for 4 to 9, there is significant jump in the net particles surface charge magnitudes from (-0.97 mC/m^2 to -2.26 mC/m^2), (-2.5 mC/m^2 to -6.66 mC/m^2) for 0.001 and 0.01 M NaCl respectively, that would reflect the influence of (pH) on the outcomes of the particles surface charge density.

The evaluated membrane particles surface charge density determined from the present study is compatible with the previous study done by Hurwitz et al. **Hurwitz, et al., 2010**. Their results showed that for electrokinetic (zeta) potential of (20.6 mV), the related surface charge was equal to (-5.0 mC/m^2) for 0.01 M NaCl, while in the present study, for a measured membrane particles zeta potential of (-18) mV, the related evaluated membrane particles surface charge was (-4.1 mC/m^2) which can prove the uniformity of the determined outcomes of this study compared with Hurwitz et al. study. This consistency in outcomes between the above two works means that they were compatible in other important determined factors such as the Debye length (K^{-1}) magnitude for (1:1) electrolytes, that was originally evaluated in this study depending on a simplified Graham formula which represents the diffuse layer thickness in the electrical double layer theory.

4.4.2 Evaluation of Effective Membrane Charge

The net charge density of the membrane (X^m) at the shear plane was estimated depending on (the Gouy-Chapman and Graham equations). So, the evaluated surface charge of membrane particles can be then transformed to concentration units by using **Eq. (4)**. The fixed charge density (X^m) of the membrane particles represents the concentration of electrical charged on the membrane particle surface in (mol/m^3).

Eq. (4) assumes that the surface charge of the membrane particles is uniformly distributed in the void volume of pores. It is important to mention that in this equation, the effective membrane surface pore radius (r_p) for the tubular ceramic titanium dioxide membrane used in this study is equal to 0.56nm (depending) on pore radius evaluated from (DSPM) model.

Fig. 11 shows an evaluated effective membrane charge density (X^m) in (mol / m^3) over a range of (pH) magnitudes from 3 to 9 using (0.001 and 0.01 M NaCl) as a background electrolyte for a 0.9 nm tubular ceramic titanium dioxide nanofiltration membrane. In order to determine the effective charge density (X^m) for the membrane in (mol/m^3), the estimated membrane particles surface charge (σ^s), (mC/m^2) should be subsequently transformed to concentration unites (x^m), (mol/m^3). It is important to mention this can be done with the assumption that the surface charge of membrane particles is uniformly distributed in the void volume of the pores.

The effective charge of the membrane particles is really representing the electrical charge groups concentration on the membrane particles in (mol/m^3), The results from **Fig. 11** show that at (pH=3), the effective membrane particles charge was equal to (22.95 mol/m^3), (46.8mol/m^3) related to surface charge density (0.55mC/m^2), (0.78 mC/m^2) for (0.001 and 0.01 M NaCl)

respectively, while at pH (9), the effective of the membrane charge particles was equal to (-93.68mol/m^3), (-276.18mol/m^3) related to the surface charge density (-2.26mC/m^2), (-6.66mC/m^2) for (0.001 and 0.01 M NaCl) respectively. It can be readily realized that this factor is also dependent on (pH) value. In the present study, the Donnan potential magnitudes in (mV) were calculated from Chein formalism, **Eq. (9)** depending on the magnitudes of the effective membrane particles charge (x^m) in (mol/m^3) for bulk concentration $C_{i,bulk}$ of 0.001 and 0.01 M sodium chloride solution. **Fig. 12** shows the evaluated Donnan potential in (mV) estimated from the effective membrane particles charge over an extent of pH magnitudes from 3 to 9 using 0.001 and 0.01M sodium chloride as a background electrolyte for a 0.9 nm tubular ceramic nanofiltration membrane. Results of **Fig. 12** show that as (pH) magnitudes increase, the potential of Donnan becomes more negative; at pH (9) is equal to (-12.3mV) and (-3.66mV) for 0.001 and 0.01M sodium chloride respectively, while at a (pH) of 3 the potential of Donnan becomes positive with the values of (2.95mV) and (0.843mV) for 0.001 and 0.01M sodium chloride respectively. Obviously, the lower the concentration, the greater the Donnan potential at the same (pH). Also, the outcomes show that for the (pH) magnitudes from 4 to 9, there is a significant jump in the determined Donnan potential magnitudes from (-5. 1 mV),(-1.46 mV) to (-12.3mV), (-3.66mV) for 0.001and 0.01M sodium chloride respectively.

The determined Donnan potential magnitude achieved from the of **Pivonka, et al., 2005**, at the same background electrolyte concentration of 0.01M NaCl and at normal pH is equal to (-2.96 mV), while the Donnan potential value from the present work is equal to (-3.5 mV). The Donnan potential is basically dependent on the salt bulk concentration of feed, the concentration of effective fixed charge in the membrane (X^m), and valence of both co-ions and counter-ions. All those factors exist in **Eq. (9)**, therefore by applying this equation, a direct magnitude for Donnan potential can be determined, while the evaluation of the Donnan potential magnitudes from other two **Eq. (5)** and **Eq. (6)** requires conducting an experiment to determine the ion concentration (such as Cl^- or Na^+ in the case of using sodium chloride as a background electrolyte) in the permeate and bulk side, that may lead to getting two different magnitudes of the Donnan potential due to the variation in retention for each ion, that is certainly inexact.

5. CONCLUSIONS

In this study circular tube ceramic, 0.9 nm titanium dioxide nanofiltration membrane was used as a model based on the (ENP: extended Nernst-Plank equation). The results show that the effective pore radius of the membrane estimated equals to 0.56 nm, the effective thickness (Δx) equals to 0.8×10^{-6} m and equivalent effective thickness ($\Delta x/A_k$) equals to 2×10^{-6} m.

The effective surface charge density (σ^s) of methe mbrane (mC/m^2), the membrane effective charge (X^m), (mol/m^3) and the Donnan potential (mV) are quite distinct between two concentration (0.001 M, 0.01 M NaCl) and altered with changing pH from pH value of 3 to pH value of 9 (increasing Ψ_{Don} with increased pH). The rejection mechanism depends very much on the Donnan effect rather than the steric effect.

The high rejection of several negatively charged salts (solutes) confirmed this finding. Without a proper characterization of the membrane properties, it would not be possible to explain the rejection behavior of the salt/solutes. Apart of being effective, this method of characterization offers a cheaper alternative in understanding membranes.

REFERENCES

- Ahmad, A. and B. Ooi, 2006, *Optimization of composite nanofiltration membrane through pH control: Application in CuSO4 removal.* Separation and Purification Technology, 47(3): p. 162-172.

- Al-Naemi, Amer Naji Ahmed, 2013, Rejection and Critical Flux of Calcium Sulphate in a Ceramic Titanium Dioxide Nanofiltration Membrane, phD Thesis.

- Benavente, J., G. Jonsson, 2000, Electrokinetic characterization of composite membranes: estimation of different electrical contribution in pressure induced potential measured across reverse osmosis membranes, J. Membr. Sci. 172 ,189–197.

- Bowen, W. and A. W. Mohammad, 1998, *Characterization and prediction of nanofiltration membrane performance—a general assessment.* Chemical Engineering Research and Design, 76(8): p. 885-893.

- Bowen, W. R. and H. Mukhtar, 1996, *Characterisation and prediction of separation performance of nanofiltration membranes.* Journal of membrane science, 112(2): p. 263-274.

- Bowen, W. R. and J. S. Welfoot, 2002, *Modelling the performance of membrane nanofiltration--critical assessment and model development.* Chemical engineering science, 57(7): p. 1121-1137

- Cai, K., M. Frant, J. Bossert, G. Hildebrand, K. Liefeith and K.D. Jandt, 2006, *Colloids Surf. B Biointerfaces,* 50, 1-8.

- Chein, R., H. Chen, and C. Liao, 2009, *Investigation of ion concentration and electric potential distributions in charged membrane/electrolyte systems.* Journal of membrane science, 342(1–2): p. 121-130.
- Condom, S., A. Larbot, S.A. Younssi, M. Persin, 2004, Use of ultra- and nanofiltration ceramic membranes for desalination, Desalination 168, 207–213.

- Davies, J. T., E. K. Rideal, 1961, ed. *Electrostatic Phenomena*, Academic Press, Inc., New York and London.

- Deen, W., 1987, *Hindered transport of large molecules in liquid-filled pores.* AIChE Journal, 33(9): p. 1409-1425.

- Dukhin, S. S., R. Zimmermann, and C. Werner, 2004, *Intrinsic charge and Donnan potentials of grafted polyelectrolyte layers determined by surface conductivity data.* Journal of Colloid and Interface Science, 274(1): p. 309-318.

- Elimelech, M., J. Gregory, X. Jia and R.A. Williams, 1995, Particle Deposition and Aggregation: Measurement, Modelling, and Simulation, Butterworth-Heinemann, Oxford.

- Eriksson, P., 1988, Nanofiltration extends the range of membrane filtration, Environmental Progress 7 (1) 58–62. doi:10.1002/ep.3300070116. URL

- Garba, Y., Taha, S., Gondrexon, N., and Dorange, 1999, G., *Ion transport modeling through nanofiltration membranes.* Journal of membrane science, 160(2): p. 187-200.

- Herbig, R., P. Arki, G. Tomandl, R.E. Br¨aunig, 2003, Comparison of electrokinetic properties of ceramic powders and membranes, Sep. Purif. Technol. 32, 363–369.

- Hurwitz, G., G. R. Guillen, and E. M. Hoek, 2010, *Probing polyamide membrane surface charge, zeta potential, wettability, and hydrophilicity with contact angle measurements.* Journal of membrane science, 2252 .343 (5–2:)p. 349-357.

- Jawor, A. and E. Hoek, 2009, *Effects of feed water temperature on inorganic fouling of brackish water RO membranes.* Desalination, 235(1-3): p. 44-57.

- Johan Schaep, Bart Van der Bruggen, Carlo Vandecasteele, Dirk Wilms., 1998, Influence of ion size and charge in nanofiltration., Separation and Purification Technology 14, 155–162

- Lanteria, Y., P. Fieveta, C. Magneneta, S. Déona and A. Szymczyk, *J. Membr. Sci.*, 2011, 378, 224– 232.

- Moritz, T., S. Benfer, P. Arki, G. Tomandl, 2001, Influence of the surface charge on the permeate flux in the dead-end filtration with ceramic membranes, Sep. Purif. Technol. 25 501–508.

- Mullet, M., P. Fievet, J.C. Reggiani, J. Pagetti, 1997, Surface electrochemical properties of mixed oxide ceramic membrane: zeta potential and surface charge density, J. Membr. Sci. 123, 255–265.

- Musbah, I., D. Cicéron, A. Saboni, S. Alexandrova, 2013, Retention of pesticides and metabolites by nanofiltration by effects of size and dipole moment, Desalination 313, 51 – 56. doi:10.1016/j.desal. 2012.11.016. URL

- Narong, P., A.E. James, 2006, Sodium chloride rejection by a UF ceramic membrane in relation to its surface electrical properties Separation and Purification Technology 49, 122–129

- Peeters, J. M. M., M. H. V. Mulder, and H. Strathmann, 1999, *Streaming potential measurements as a characterization method for nanofiltration membranes.* Colloids and Surfaces A: Physicochemical and Engineering Aspects, 150(1–3): p. 247-259.

- Pessarakli, M., 1999, *Handbook of plant and crop stress* : CRC.

- Rahi, K. A., and T. Halihan, 2010, *Changes in the salinity of the Euphrates River system in Iraq.* Regional Environmental Change, 10(1): p. 27-35.

- Salgın, S., S. Takaç and H.T. Özdamar, *J. Colloid Interf. Sci.*, 2006, 299, 806-814.

- Schaep, J. and C. Vandecasteele, 2001, *Evaluating the charge of nanofiltration membranes.* Journal of membrane science, 188(1): p. 129-136.

- Schäfer, A. I., Fan A. G., and Waite T. D., 2007, *Nanofiltration principles and applications*: Elsevier.
- Silva, V.; P. Prádanos, L.P., J. I. Calvo and A. Hernandez, 2009, *Relevance of hindrance factors and hydrodynamic pressure gradient in the monetisation of the transport of neutral solutes across nanofiltration membranes.* Chemical Engineering Journal, 149: p. 78–86.
- Song, L. and M. Elimelech, 1995, Particle deposition onto a permeable surface in laminar flow, J. Colloid Interface Sci., 173, 165.
- Wang, X.L., T. Tsuru, M. Togoh, S. Nakao, S. Kimura, 1995, Evaluation of pore structure pressure reverse osmosis properties and applications, and electrical properties of nanofiltration membranes, J. Chem. Eng. Jpn. 28, 186.
- Zhu, X. and M. Elimelech, 1995, Fouling of reverse osmosis membranes by aluminum oxide colloids, J. Environ. Eng., 121 (12) 884.

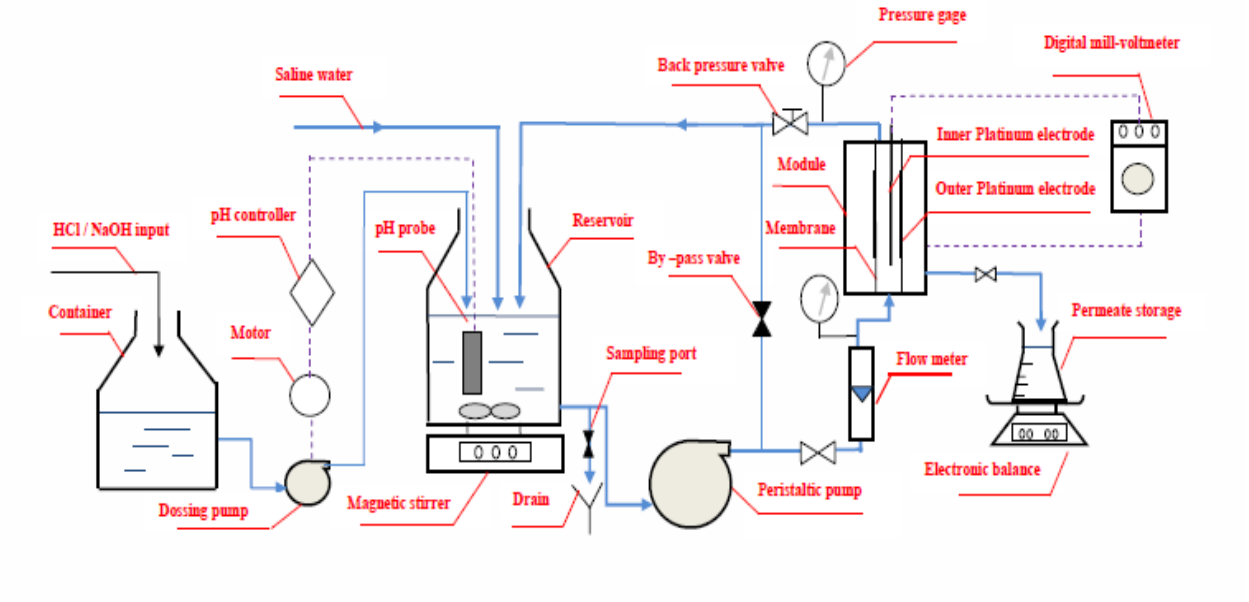

Figure 1. A Schematic diagram of TiO_2 NF membrane rig for testing flux rejection properties.

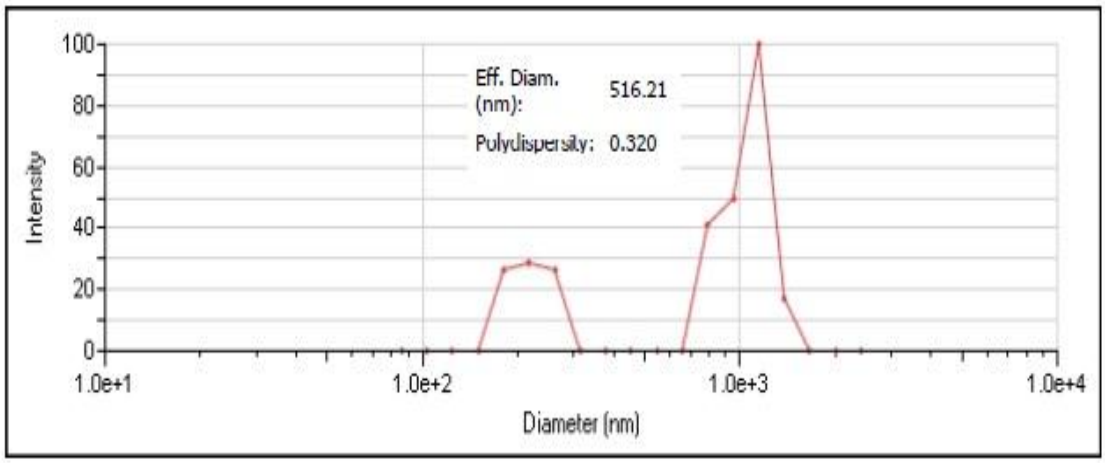

Figure 2. The effective diameter measurement of the tubular ceramic TiO_2 membrane powder with Eff. Diam. : 516 nm.

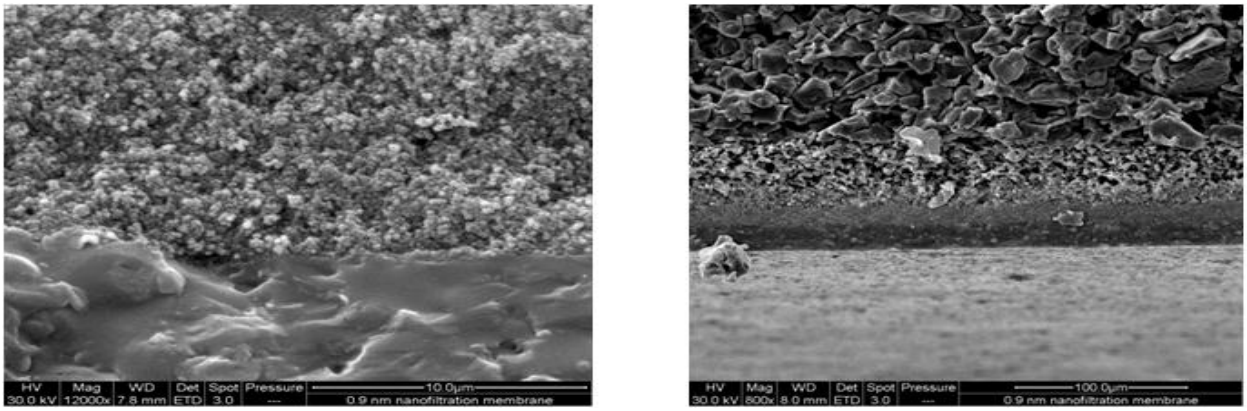

Figure 3. SEM cross-section image of 0.9 nm titanium dioxide NF membrane

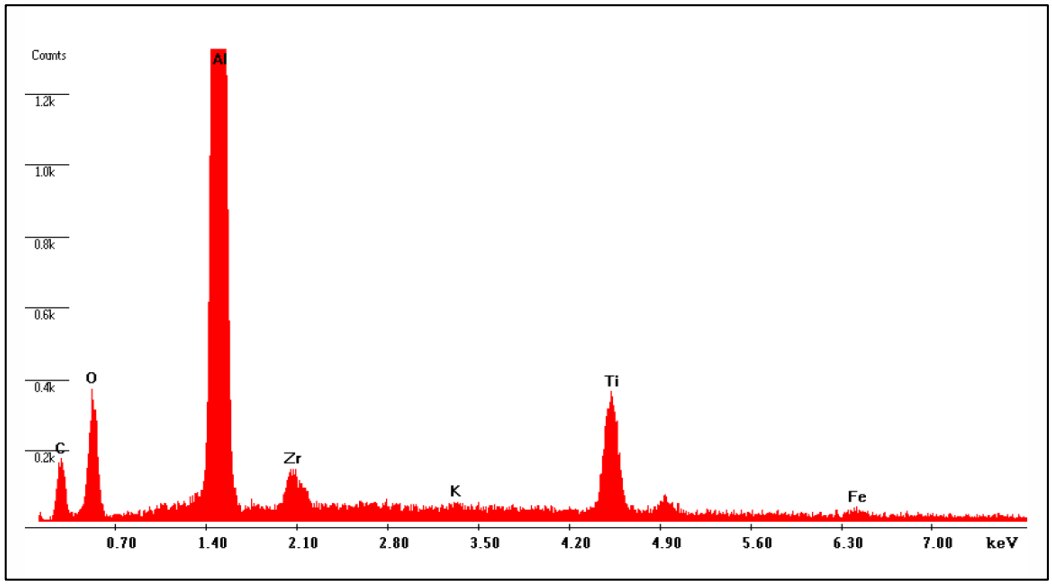

Figure 4. EDXS spectrum of 0.9 nm titanium dioxide NF membrane.

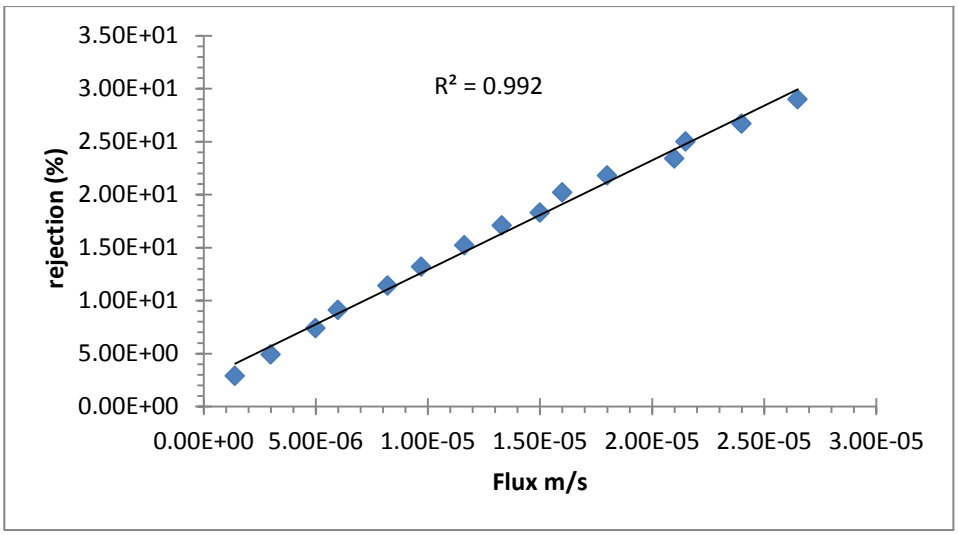

Figure 5. Rejection of glucose as a function of permeate flux for 0.9 nm (TiO_2) NF membrane.

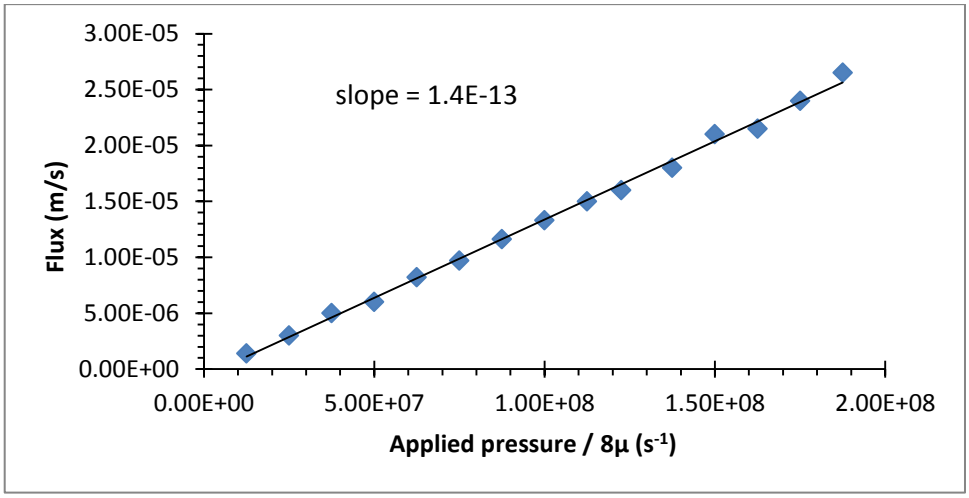

Figure 6. Permeate flux of glucose as a function of applied pressure for NF membrane.

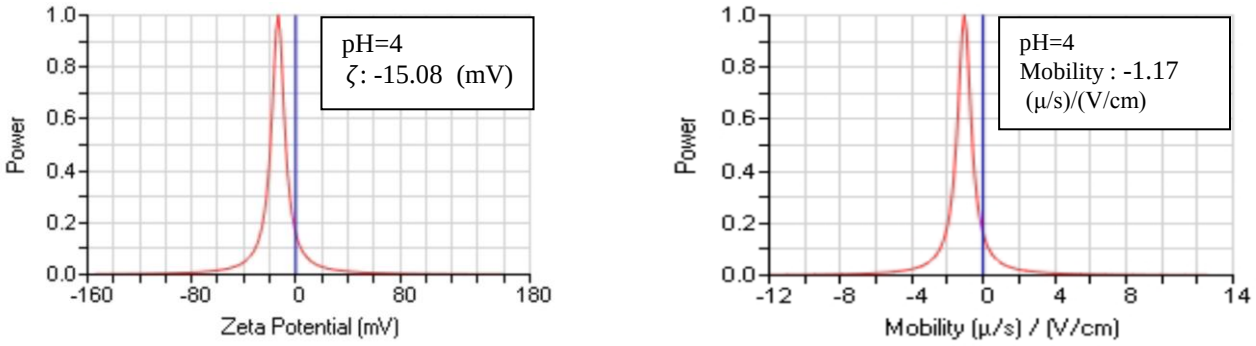

Figure 7. A sample of zeta potential measurement and mobility at 0.001 M NaCl concentration for pH 3 and 4.

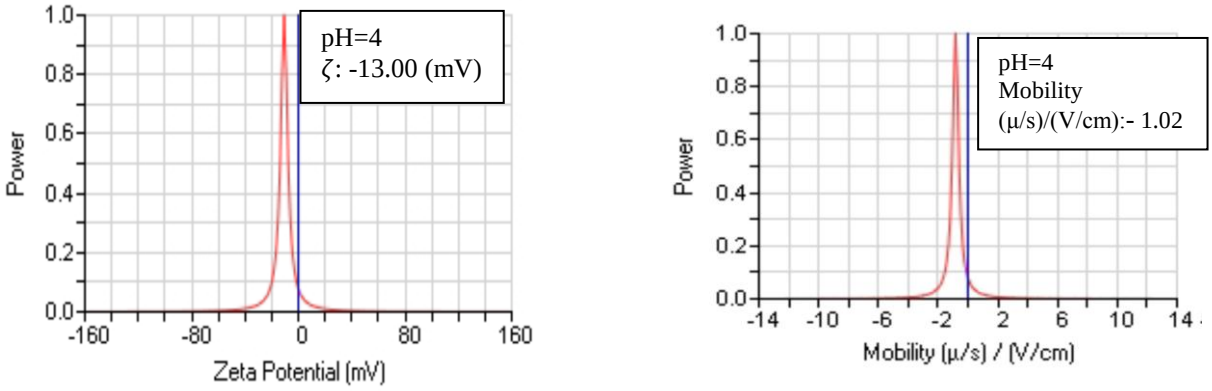

Figure 8. A sample of zeta potential measurement and mobility at 0.01 M NaCl concentration for pH 3 and 4.

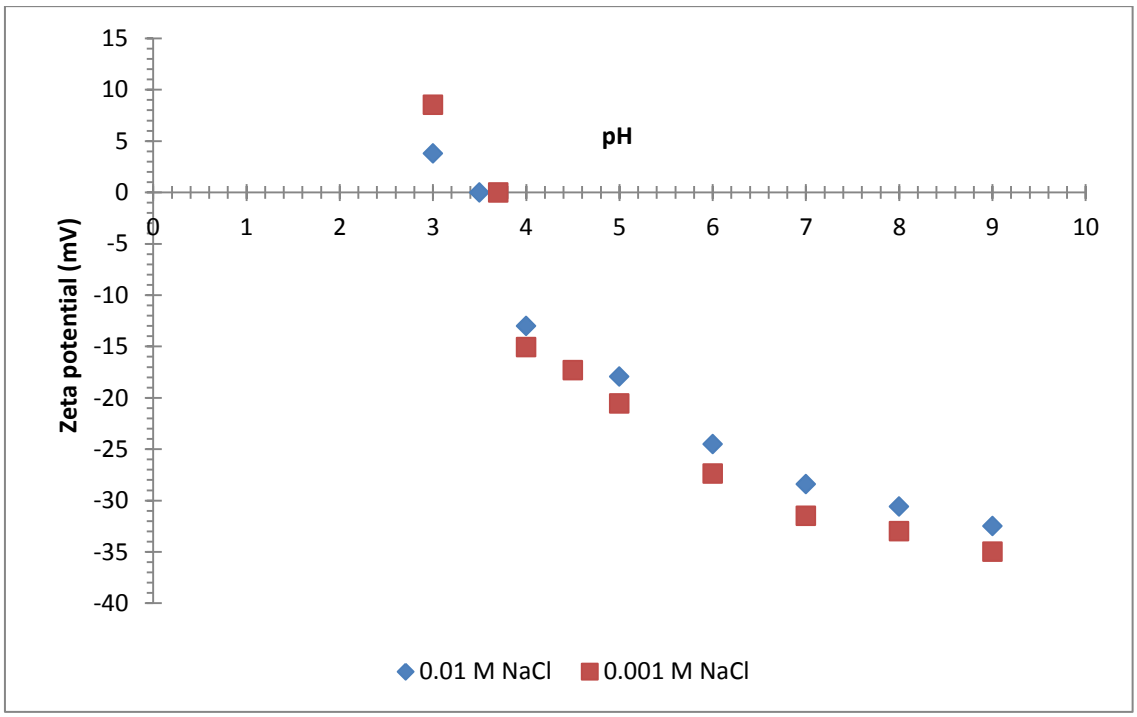

Figure 9. Zeta potential of (TiO_2) NF membrane measured micro-electrophoresis from plotted versus pH for background electrolyte of 0.001 M & 0.01M NaCl with (i.e.p.) of 3.7 and 3.5 respectively.

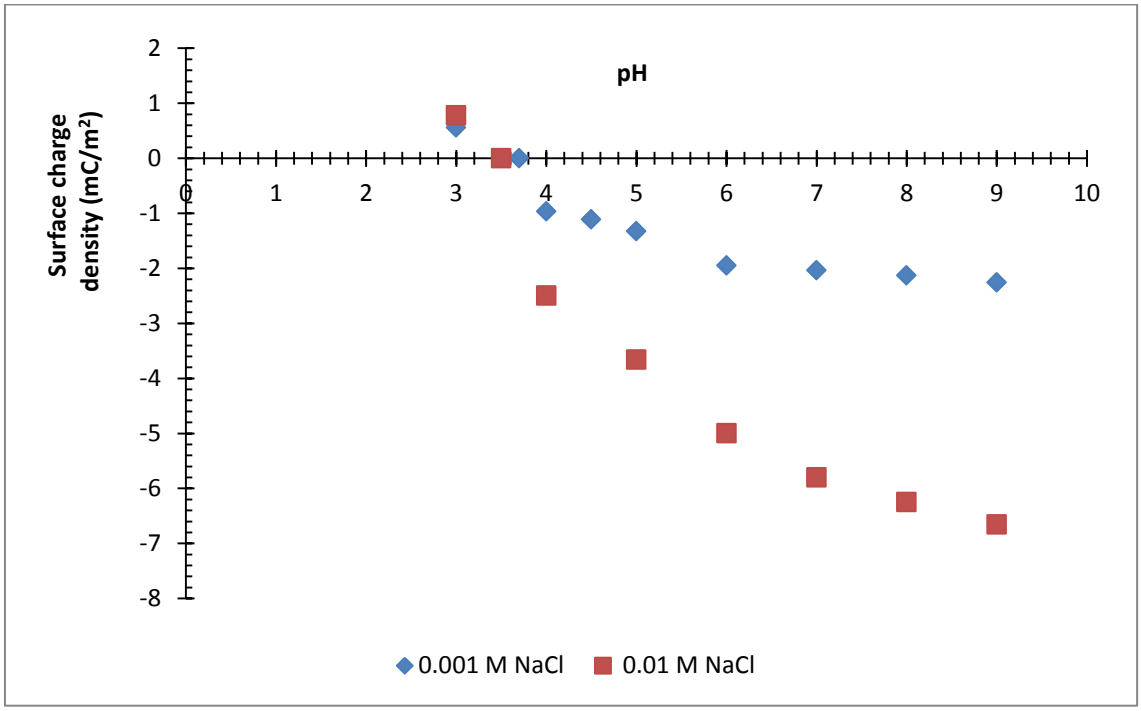

Figure 10. The surface charge density of (TiO_2) NF membrane estimated from micro-electrophoresis potential plotted versus pH for background electrolyte fixed at 0.001 and 0.01 M sodium chloride.

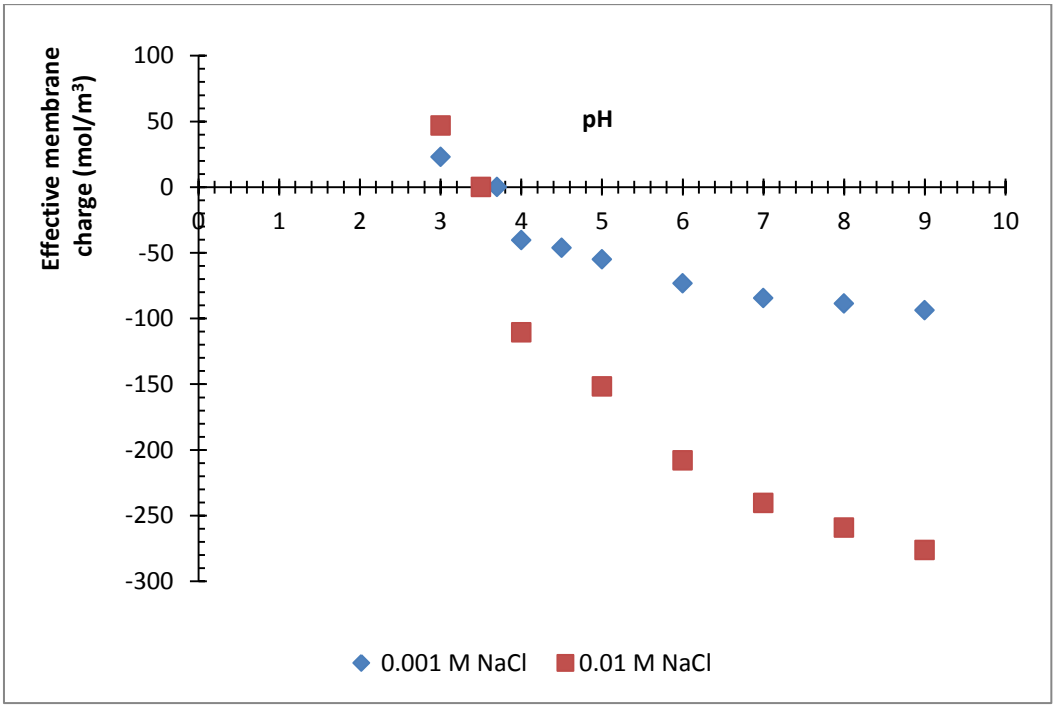

Figure 11. Effective membrane charge of NF membrane estimated from micro-electrophoresis potential plotted versus pH for background electrolyte fixed at 0.001 and 0.01 M NaCl.

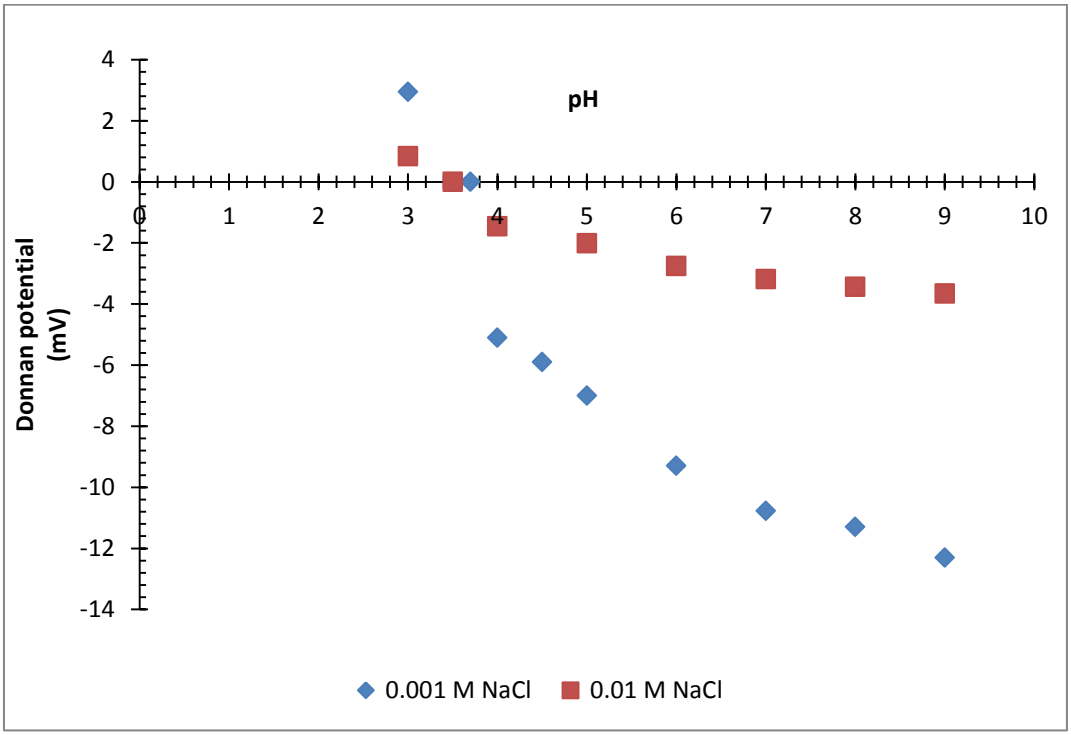

Figure 12. Donnan potential of (TiO_2) NF membrane estimated from micro-electrophoresis potential plotted versus pH for background electrolyte fixed at 0.001 and 0.01 M NaCl.